Oral epithelial cells distinguish between *Candida* species with high or low pathogenic potential through miRNA regulation

Márton Horváth[1], Gábor Nagy[2], Nóra Zsindely[1], László Bodai[2], Péter Horváth[4,5], Csaba Vágvölgyi[1], Joshua D. Nosanchuk[6], Renáta Tóth[1,†], Attila Gácser[1,3,†,#]

[1] Department of Microbiology, University of Szeged, Szeged, Hungary

[2] Department of Biochemistry and Molecular Biology, University of Szeged, Szeged, Hungary

[3] MTA-SZTE Lendület Mycobiome Research Group, University of Szeged, Szeged, Hungary

[4] Synthetic and Systems Biology Unit, Biological Research Centre (BRC), Szeged, Hungary.

[5] Institute for Molecular Medicine Finland, University of Helsinki, Helsinki, Finland

[6] Departments of Medicine (Infectious Diseases) and Microbiology and Immunology, Albert Einstein College of Medicine, Bronx, New York

[†] These authors share last authorship.

[#]Address correspondence to Attila Gacser, gacsera@bio.u-szeged.hu

Running Head: Host miRNA responses distinguish between *Candida* species

Major subject areas: Molecular biology, Microbiology and Infectious Disease, Immunology

Keywords: *Candida*, oral epithelial cell, host-pathogen interaction, miRNA regulation

Research organism(s): *Candida albicans*, *Candida parapsilosis*

Impact statement: Altered miRNA regulation discriminates between *C. albicans* and *C. parapsilosis* in human oral epithelial cells

Abstract

Oral epithelial cells monitor microbiome composition and initiate immune response upon dysbiosis, as in case of *Candida* imbalances. Comparison of healthy oral epithelial cell responses revealed that the inability of *C. parapsilosis* to induce a robust antifungal response was due to activation of various inflammation-independent pathways, while *C. albicans* robustly activated inflammation cascades. Regarding posttranscriptional regulation, several miRNAs were altered by both species. For *C. parapsilosis*, the applied dose directly correlated with changes in transcriptomic responses. Carbohydrate metabolism, hypoxia- and cardiovascular development-related responses dominate after *C. parapsilosis* stimulus, whereas *C. albicans* altered inflammatory responses. Subsequent analyses of HIF1-α and HSC-activation pathways predicted target genes through which miRNA-dependent regulation of yeast-specific functions may occur, supporting the observed responses. Thus, *C. parapsilosis* is recognized as a commensal at low doses by the oral epithelium; however, increased fungal burden activates different pathways, some of which overlap with inflammatory processes induced by *C. albicans*.

Introduction

The barrier function of epithelium is of paramount importance in maintaining homeostasis and protecting hosts against an array of injuries, including from microbes. Besides providing physical protection, cells of the epithelium produce and secrete various enzymes (e.g., lysozymes), peptides (e.g., defensins), and other small molecules (e.g., free oxygen radicals) that inhibit or kill diverse microbes (1). Epithelial cells also actively contribute to innate immune responses (2). Opportunistic pathogenic *Candida* species are members of the normal human mucosal microflora of the oral cavity, airways, intestinal tract and genitals (3). These species primarily cause infections in immunosuppressed patients or individuals with disrupted barrier functions (4). When *Candida* are able to avoid or subvert host responses, serious and persistent local or systemic infections can arise (collectively also referred to as candidiasis), which includes life-threatening invasive infections (5). The most common species associated with systemic invasive candidiasis is *C. albicans*, although the occurrence of *non-albicans Candida* (NAC) species has risen sharply in recent years, and invasive infections from NAC species are more frequent than *C. albicans* in many geographical regions (6)(7).

One of the most common forms of candidiasis is oral candidiasis, which is primarily caused by *C. albicans* followed by *C. glabrata*, *C. parapsilosis*, *C. tropicalis*, and *C. pseudotropicalis* (8). All of these species may be present in the healthy oral mycobiome; however, their amount and diversity increases upon dysbiosis due to inflammation or cancer (9)(10). These conditions also significantly increase the risk of developing oral candidiasis. Recent cohort studies suggest that oral candidiasis occurs in ~ 32% of organ transplant patients (11), ~ 36% of diabetic patients (12), 55% of patients with radiation-induced stomatitis (13), and ~3 to 88% of individuals infected with HIV, depending on the geographical location (14).

Interactions between oral epithelial cells (ECs) and *C. albicans* are widely studied. In *C. albicans*, the most important step of the commensal-to-pathogen conversion is the yeast to hyphae morphology shift. Hypha-associated proteins enable the fungus to acquire trace elements (e.g. iron) from ECs, attach to host cells and invade through the epithelial barrier via induced endocytosis or active penetration (15)(16). Once adhered to the host's surface, fungal cells are recognized mainly by Toll-like receptors and C-type lectin receptors, which activate various signaling pathways (NF-κB, and MAPK signaling). Epithelial damage also occurs, due to the secretion of various fungal enzymes or toxins, including Candidalysin (17). As a result, a shift in the host biphasic-MAPK signaling occurs, which discriminates between the

commensal and pathogenic state of *C. albicans* (18). In contrast, relatively little is known about EC responses to NAC species, such as *C. parapsilosis*. This is important as the pathobiology of these two species are extremely different. For example, *C. albicans* elicits an almost immediate and vigorous proinflammatory host responses, while the response evoked by *C. parapsilosis* is mild and delayed (19). The milieu of the colonization site also seems to greatly influence the host response towards these species given the previous findings that (i) in contrast with *C. albicans*, *C. parapsilosis* is a common natural commensal of the human skin (20,21), and (ii) *C. parapsilosis* infrequently causes oral candidiasis (22,23) One possible explanation for the markedly different host responses may be due to differences in posttranscriptional regulatory processes. microRNAs (miRNAs) are important players in fine-tuning the expression of genetic information. Recent studies demonstrate several pathogen associated molecular pattern (PAMP)-inducible miRNAs as well as miRNAs activated by TLR signaling, such as miR-155, miR-132, miR-125b or miR-146a (24), that exhibited altered expression upon bacterial or viral induction (25). Despite their confirmed relevance in host-pathogen interactions, only a few studies have analyzed miRNA profiles of host cells following *C. albicans* exposure. According to these investigations, miR-146 expression was significantly increased following β-glucan (a cell wall component of *C. albicans* cells) treatment in THP-1 cells, which resulted in the inhibition of the proinflammatory response (26). Heat-killed *C. albicans* were found to increase expression of 5 miRNAs in macrophages, including miR-155 and miR-146a, and the changes were induced by the activation of NF-κB signaling (27). In terms of epithelial barriers, the presence of *Candida*-reactive miRNAs has also been reported in airway ECs where several miRNA species associated with, for example, cell division, apoptosis or differentiation processes, were identified (28).

In this study, we aimed to investigate how healthy oral ECs discriminate between *C. albicans* and *C. parapsilosis*, and to dissect the potential underlying discriminatory mechanisms of the detected host responses. We further sought to examine whether species-specific posttranscriptional regulatory processes controlled the phenomenon by performing in-depth *in silico* analyses of both transcriptomic and miRNA sequencing data.

Results

Robust antifungal humoral response is triggered by *C. albicans*, but not *C. parapsilosis* in oral epithelial cells

In contrast with other innate immune cells, direct cellular responses, such as pathogen internalization and subsequent killing, are not a major function of ECs. This was reflected by the extremely low interaction events between *Candida* and ECs when examining direct cell-cell interactions, which were too few to allow the authentic interpretation of data (data not shown). Rather, the function of ECs manifests in the activation of professional phagocytic cells through the secretion of chemokines, cytokines or other signaling molecules. Additional responses include the secretion of antimicrobial peptides, such as beta-defensins, another route to effectively combat invading pathogens (29,30). To investigate the nature of healthy oral epithelial humoral responses to *C. albicans* and *C. parapsilosis*, OKF6/TERT2 cells were used. We first examined the host cell damaging capacity of both yeast species (FIG 1/A). For subsequent analyses, infection doses were selected that did not exceed 25% of host cell damage. For *C. albicans*, the multiplicity of infection (MOI) of 1:1 met this criterion (22.09 ±3.23%), while none of the applied *C. parapsilosis* doses resulted in a more than 10% of host cell loss. Therefore, we selected the highest infection dose, which is in accordance with the literature (31–33). Next, we investigated the expression of proinflammatory (TNF-α, IL-1α/β, and IL-6) and immunoregulatory (GM-CSF) cytokines, chemokines (IL-8, ccl2, ccl20) and an antimicrobial peptide (human β-defensin 2, or hBD-2). Remarkably, *C. albicans* elevated the expression of all examined chemokines and cytokines (from 7 to 840 times higher expression) relative to the untreated control (FIG 1/B). Co-culture with *C. parapsilosis* also resulted in statistically significant differences in cytokine/chemokine responses; however, compared to the exuberant immune response evoked by *C. albicans*, these changes were modest (FIG 1/B). For *C. parapsilosis*, these included IL-1α (2.21±0.65, $p=0.097$), IL-1β (1.65±0.11, $p<0.01$), ccl2 (0.52±0.1, $p<0.01$) and CSF2 (3.12±0.53, $p<0.05$), relative to the untreated sample's normalized value of 1. Although not significant, the expression of hBD-2 increased in the presence of *C. albicans* only (FIG 1/C). Hence, we found marked differences in the immune response triggered by the two *Candida* species. Next, we aimed to examine whether these distinctive responses were due to alterations in regulatory processes during stimulation with these fungi.

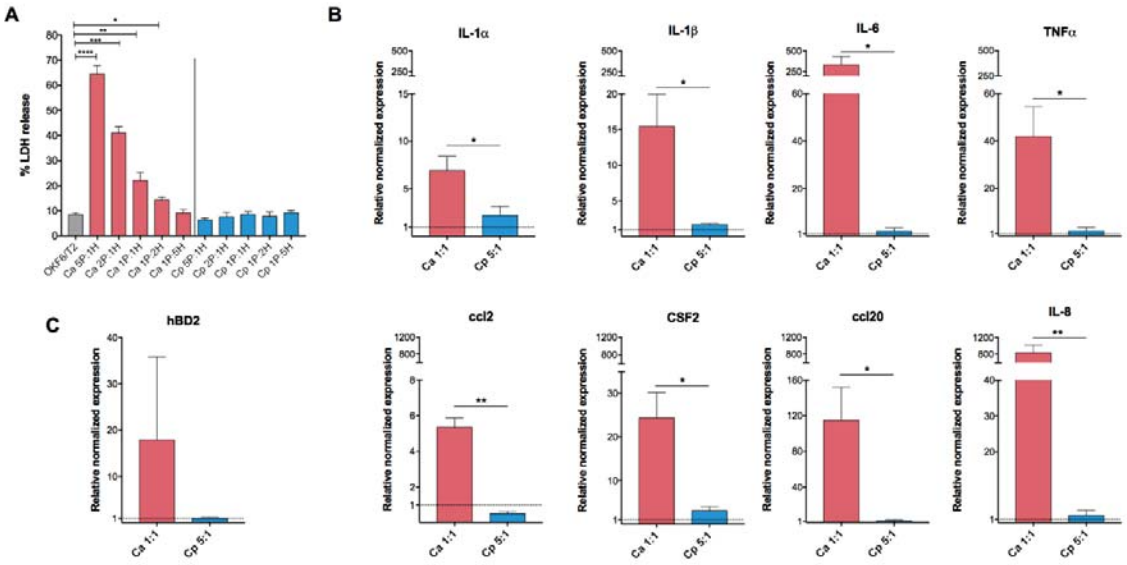

155

156 **FIG 1 - Epithelial response activation by *C. albicans* and *C. parapsilosis*.** OKFT6/TERT2 cells were cultured
157 with *C. albicans* or *C. parapsilosis* in different infection ratios to investigate their host cell damaging capacity
158 and EC responses after 6 hours of coincubation. (A) Host cell damage was assessed by lactate dehydrogenase
159 (LDH) measurement. Relative normalized expression of cytokine and chemokine encoding genes (B) and the
160 human beta defensin 2 (hBD2) encoding gene (C) were determined by qPCR. The depicted significance defines
161 the differences between the two fungal treatments. Data were normalized to the uninfected control values (set at
162 equal to 1). Data were obtained from three independent experiments (n=3), and analyzed by unpaired t-tests. (*,
163 $p < 0.05$; **, $p < 0.01$; ***, $p < 0.001$; ****, $p < 0.0001$)

164

165 **Species-specific host gene- and miRNA expression profiles detected towards *C.**
166 ***parapsilosis* and *C. albicans***

167 Transcriptome and miRNA profile analyses were performed to further examine the distinctive
168 responses of the ECs to the two yeast species. To obtain analysis-ready count data from the
169 raw sequencing result files, we followed the pipeline detailed in FIG 2/A. In addition to the
170 abovementioned doses for the two species (MOI 1:1 for *C. albicans*, and 5:1 for *C.*
171 *parapsilosis*), we also applied the dose 1:1 for *C. parapsilosis* for the subcellular analyses in
172 order to have an equivalent ratio of host-pathogen for comparisons. Transcripts were analyzed
173 both after an early (1h) and a later (6h) time point of fungal exposure to further examine both
174 inflammatory, as well as potentially activated non-inflammation-related EC responses. These
175 data were compared to that of the uninfected controls. Our results indicate that the majority of
176 host cell responses to both species occurred 6 hours after the start of the co-culture, rather
177 than shortly following the initial interactions (FIG 2/B). When comparing the MOI 1:1
178 infection doses of both species at 1 hour of co-culture, 50 differently expressed genes (DEGs)

were identified with 46 (20 down-, 26 upregulated) occurring in *C. albicans* and 4 (all downregulated) in *C. parapsilosis* treated cells. At the 6 hour time point, 648 DEGs (348 down-, 259 upregulated) were identified in the setting of ECs with *C. albicans* and 79 (23 down-, and 56 upregulated) with *C. parapsilosis*. Thus, at both time points, *C. parapsilosis* treatment effected the expression of a significantly lower number of genes at the MOI of 1:1. Once the fungal load was increased however (MOI 5:1), significantly more DEGs were identified at both times (83 DEGs at 1 hour: 23 down-, 60 upregulated; and 262 DEGs at 6 hours: 55 down-, 207 upregulated), which exceeded the number of DEGs identified after *C. albicans* stimulus at 1 hour. During the transcriptome analysis, we identified genes with species-specific expression, and identical genes with similar or opposite expression patterns when comparing *C. albicans* and both ratios of *C. parapsilosis* (FIG 2/B). The identified DEGs under the different conditions are listed in Table S2.

Next, we examined the ECs' miRNA profile. miRNA analysis results revealed several miRNAs that were specifically expressed not only in the presence of the two species but also specific to the applied doses of *C. parapsilosis*. We identified 2, 2 and 3 mature miRNA transcripts at 1 hour and 2, 8 and 16 at 6 hours of *C. parapsilosis* MOI 1:1, MOI 5:1 and *C. albicans* MOI 1:1 stimulus, respectively (FIG 2/C). While the majority of miRNAs showed a condition-specific altered expression, miR-4464-3p showed a significantly increased expression at 1 and 6 hours of *C. albicans* treatment compared to the untreated control. Of the differentially expressed miRNAs, 1, 2 and 2 target mRNAs were found at 1 hour, while 12, 56 and 185 target mRNAs were identified at 6 hours of *C. parapsilosis* MOI 1:1, MOI 5:1 and *C. albicans* MOI 1:1 stimulus, respectively (Table S3-5). These results suggest that species-, and in case of *C. parapsilosis*, dose-specific posttranscriptional regulatory mechanisms regulate host responses under the applied conditions, which could explain the altered transcriptomic responses.

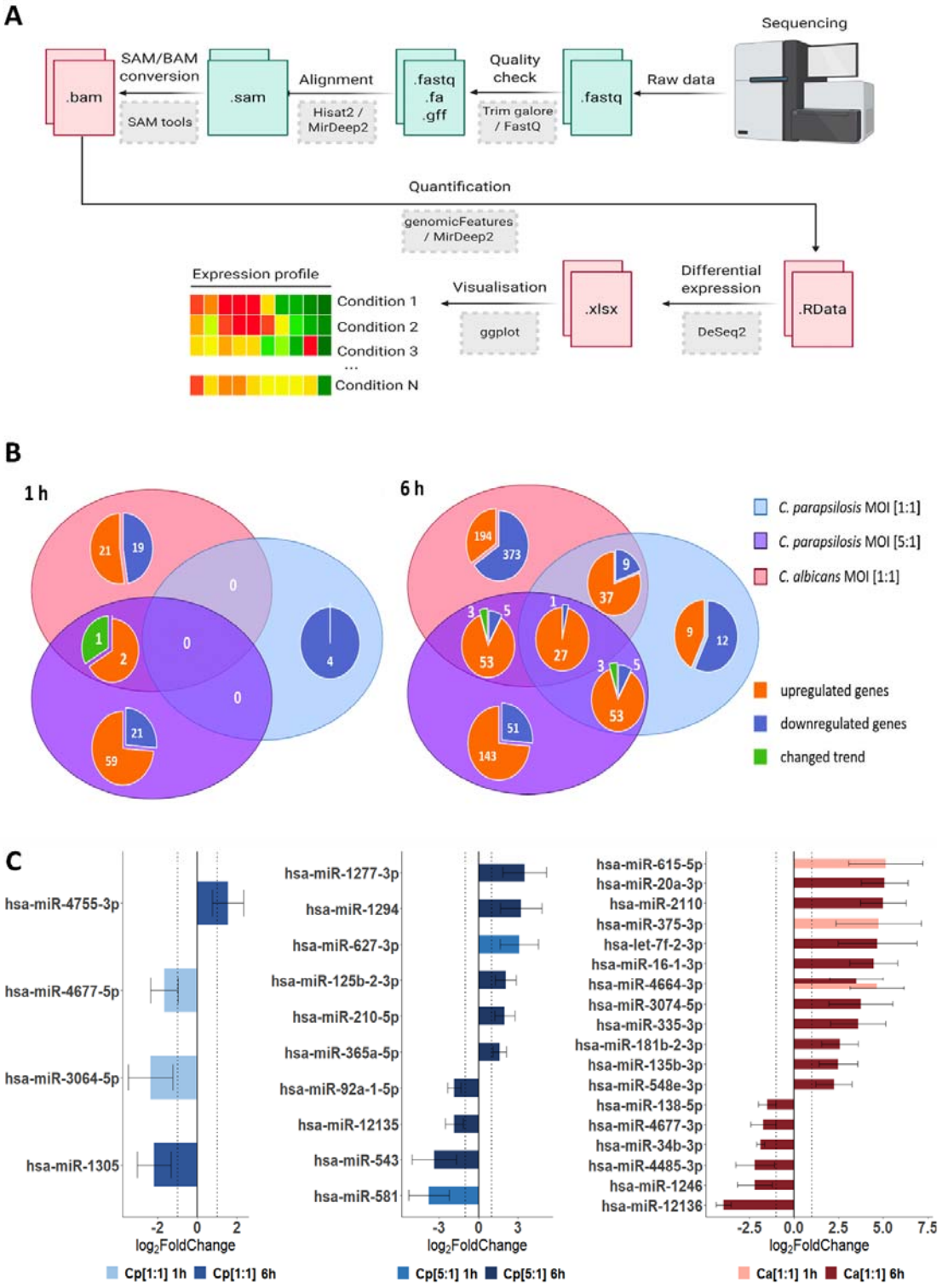

FIG 2 - Differentially expressed genes (DEGs) and dysregulated miRNAs in host responses following fungal stimuli. Host transcriptomic and miRNA responses were examined with NGS sequencing methods (Illumina). (A) Workflow of raw data analysis, where the obtained sequences were processed alongside the above detailed bioinformatical pipeline via command line (perl- and java-based) bioinformatical tools (grey

boxes), through the listed intermediate files (green/red boxes). (B) Venn-diagrams of host genes identified at 1 and 6 hours under each applied condition. Numbers of condition specific genes as well as genes regulated by multiple conditions are shown. The term 'changed trend' (green) refers to genes regulated by more than one condition, but the fold change was positive under at least one condition and negative in another. (C) Differently expressed host miRNA profiles after the applied conditions.

Carbohydrate metabolism-, hypoxia- and cardiovascular development-related responses dominate after *C. parapsilosis* stimulus, while *C. albicans* predominantly induces inflammation responses

Next, we aimed to categorize the identified transcripts and characterize host responses based on the activated host signaling pathways. We employed different GSEA and ORA methods (FIG 3/A) to examine the modified canonical pathways (KEGG's pathway analysis, Figure 3/B) and biological functions based on gene ontologies (GO term analysis, FIG 3/C). At 1 hour after fungal exposure, the responses detected did not allow for a more in-depth analysis. Therefore, we focused on the 6-hour data set. With *C. albicans* treated ECs, both biological pathways and functions were clearly dominated by inflammatory responses as shown by the ten most activated pathways and functions in FIG 3/B-C. Some of the most significantly regulated pathways were the cytokine-cytokine receptor interaction, tumor-necrosis factor (TNF) signaling, and IL-17 signaling pathways, while activated biological functions included inflammatory responses, responses to bacteria, to molecules of bacterial origin (e.g. LPS) and to chemokines (Table S6-7). In contrast, *C. parapsilosis* 1:1 infection resulted in the activation of routes involved in cardiovascular development and, interestingly, pathways frequently associated with carcinogenesis (e.g. Rap1 and Ras signaling pathways, HIF1 and VEGF signaling pathways). The affected biological pathways dominantly clustered around cardiovascular development (e.g. vasculature development or angiogenesis) (Table S8-9). Similar pathways were also activated by the *C. parapsilosis* MOI 5:1 co-culture, although these were also complemented with activations of carbohydrate metabolic pathways (e.g. starch and glucose metabolism pathways) and hypoxia-related response routes (e.g. HIF1-α signaling pathway). Co-culture of ECs with *C. parapsilosis* at MOI 5:1 also induced the activation of a few inflammation-related pathways (e.g. cytokine-cytokine-R interaction pathway) (Table S10-11). Thus, while *C. albicans* triggered multiple inflammation pathways, *C. parapsilosis* evoked a variety of mainly inflammation-independent host responses that have not been previously associated with this species.

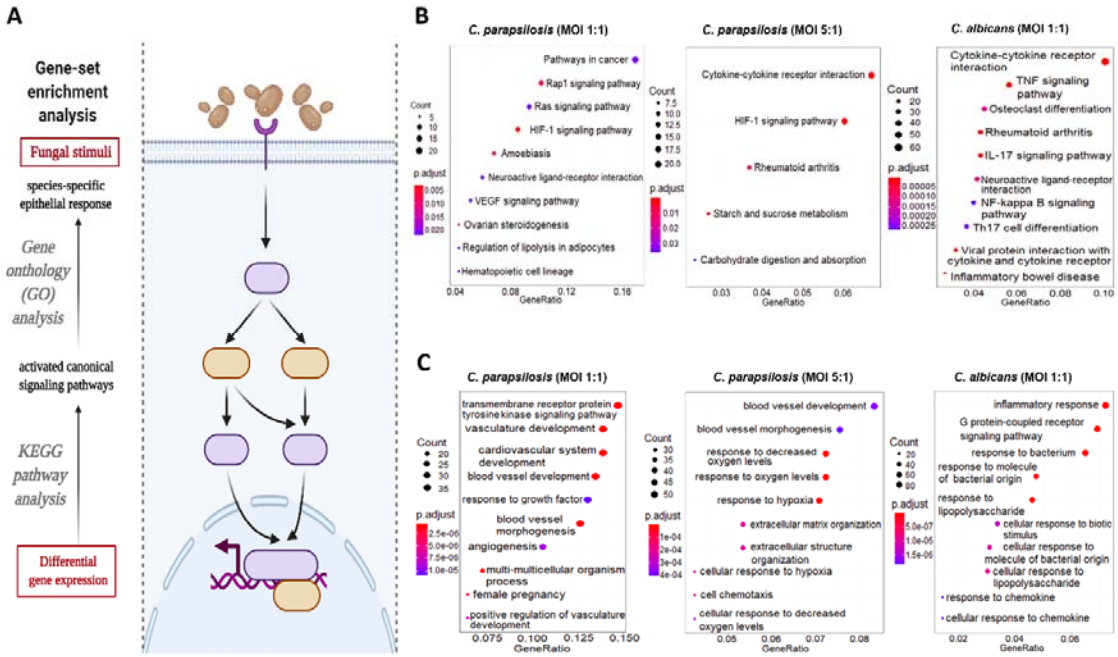

FIG 3 - Results of the KEGG pathways and GO term analyses. (A) The 'enrichKEGG' and 'enrichGO' functions (provided within the R-package – DOSE) – and 'CNA', and 'URA' analyses (provided within Ingenuity Pathway Analyses methods) were used to analyze the significantly up/downregulated pathways, functions, and upstream regulatory networks, respectively. (B-C) – List of the 10 most activated pathways and functions after each stimuli (B). The KEGG results were labelled with their respective interest-to-background ratio (x-axis on the figures) within the pathways, their significance (color-coding) and with a corresponding 'count', which refers to the number of DEGs within a specific pathway. 10 (or less) significant pathways with the biggest 'Gene Ratio' were visualized as dotplots via the 'enrichplot' package. (C) The GO term results were visualized similarly for all the applied conditions.

Potential effects of species-specific miRNA responses on host cell function

To examine whether the identified miRNAs could affect the evoked transcriptomic responses, we first overlapped the targets of the obtained miRNAs and the corresponding altered transcriptomic profiles in each condition. Then, using cluster analyses of GO overrepresentation tests, we analyzed functions that the potential target mRNAs (or the target genes of all identified miRNAs per condition) could affect under each condition. As the early transcriptional responses under all conditions and the later transcriptional responses after *C. parapsilosis* MOI 1:1 treatment were only mild, none of the predicted functions passed the set p value threshold. Thus, only the differentially expressed target mRNAs derived from *C. parapsilosis* MOI 5:1 and *C. albicans* MOI 1:1 stimuli were analyzed (FIG 4/A-B). According to the GO term analyses, the top 5 target mRNA functions of target mRNA functions after *C. albicans* challenge were ‘response to bacteria’, ‘regulation of metabolic processes’, ‘negative regulation of cell proliferation’, ‘response to hypoxia’ and ‘multicellular processes’ ($p<0.0001$) (FIG 4/A, Table S12). These were clustered in the following categories: ‘response to stimulus’, ‘metabolic processes’, ‘cellular processes’ and ‘developmental processes’, respectively. With *C. parapsilosis* co-culture, 'response to hypoxia’, ‘positive regulation of chemotaxis’, ‘vascular processes’, ‘positive regulation of migration’ and monosaccharide metabolic processes’ were listed as the most significantly enriched functions ($p<0.0001$), within the major identified clusters of ‘response to stimulus’, ‘cell motility, ‘developmental processes’, and ‘metabolic processes' (FIG 4/B, Table S13). These data suggest that the identified miRNAs could actively regulate the identified species-specific transcriptomic responses.

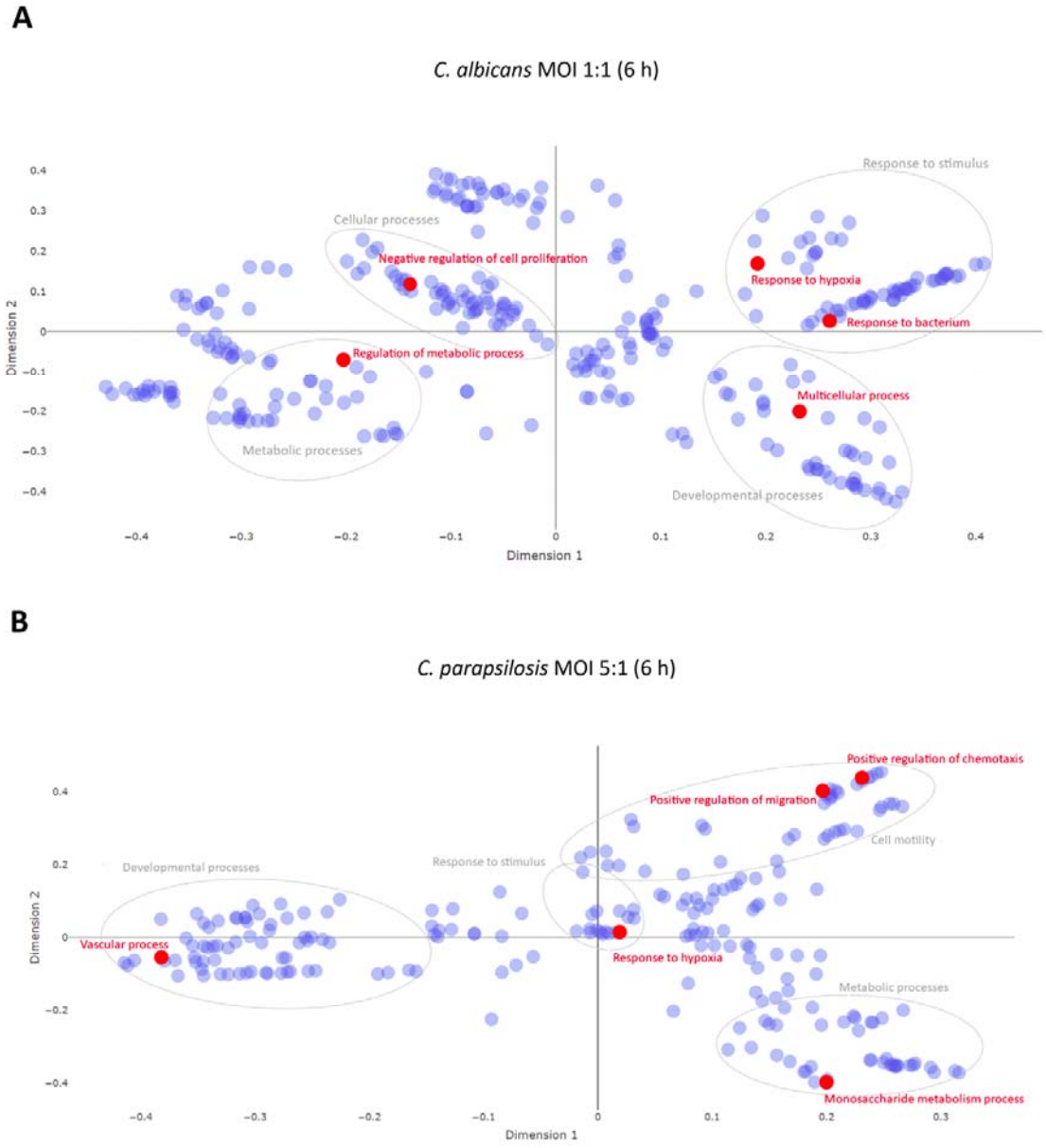

277

278

279 **FIG 4 - Multidimensional Scaling plot of target mRNA functions**. Potential effects of condition-specific
280 miRNAs on transcriptomic responses. The potential functions of target mRNA were analyzed using cluster
281 analyses of GO overrepresentation tests. Top 5 functions (shown in red) of target mRNAs at 6h *C. albicans* MOI
282 1:1 treatment (A) and *C. parapsilosis* MOI 5:1 challenge (B). Grey circles represent the corresponding clusters
283 of each highlighted functions.

284

285

HIF1-α-pathway activation results in disrupted glucose metabolism after *C. parapsilosis* stimulus, and survival promotion after *C. albicans* infection

In addition to the several species-specifically activated signaling pathways, we found two - HIF1- α and hepatic stellate cell (HSC) activation signaling pathways - that were significantly regulated in all three experimental setups at 6 hours. Therefore, we examined these pathways in more depth. In the HIF1-α-pathway, the *C. parapsilosis* MOI 1:1, MOI 5:1 and *C. albicans* MOI 1:1 stimuli resulted in the significant up- or downregulation of 7, 11 and 15 genes, respectively. In each case, we found treatment-specific activated genes as well as genes whose expression altered under at least two conditions (FIG 5/A). The HIF1-α-signaling pathway was significantly activated during all three types of stimuli compared to the 'basal expression' level of the unstimulated cells. The effect was statistically most significant after the *C. parapsilosis* 5:1 treatment (p = 3.32e-08), followed by *C. parapsilosis* MOI 1:1 (p = 3.99e-07) and *C. albicans* MOI 1:1 (p= 1.19e-06) (FIG 5/B). We next examined potential functions that could be altered with HIF1α-pathway deregulation. A similar activation pattern was observed in three of these biological processes: cell survival, migration, and angiogenesis. *C. albicans* clearly activated these processes (z-scores: 3.781, 3.185 and 3.481 of cell survival, migration, and angiogenesis, respectively), while the *C. parapsilosis* MOI 5: 1 treatment resulted in a similar effect, but activation occurred to a lesser extent (z-scores: 3.060, 2.789 and 3.879, respectively). The *C. parapsilosis* MOI 1: 1 stimulus led to only mild activation or even inhibition (z-score of survival: 1.601, angiogenesis: 0.860, migration: -0.19). Furthermore, extracellular matrix (ECM) synthesis inhibition was a characteristic of *C. albicans* treatment, while activation of glucose uptake and metabolism was a unique effect of the two *C. parapsilosis* stimuli (FIG 5/C).

Next, we aimed to examine potential correlations between the results of the transcriptome and miRNA analyses by identifying miRNA-target mRNA pairs. Such pairs were identified after both *C. albicans* and *C. parapsilosis* MOI 5: 1 co-culture, but none were found for the *C. parapsilosis* MOI 1: 1 condition (Figure 5 / D).

For *C. albicans*-treated ECs, miR-34b (downregulation, LFC= -1.87) and its potential target mRNA, TGF-α (transforming growth factor alpha; upregulation, LFC = 1.758) – a known regulator of cell proliferation and survival - was identified. Another miRNA-mRNA pair included miR-2110 (LFC= 5.00) and PIK3R3 (phosphoinositide-3-kinase regulatory subunit 3; LFC= -2.53). In the case of *C. parapsilosis* MOI 5:1-treated ECs, miR-210 (LFC = 1.98) and its potential target CAMK2B (calcium-dependent protein kinase 2 beta; LFC= -2.36) and another miRNA, miR-92a (LFC= -1.85) were identified. The latter's potential HIF1-α-

pathway target elements include: EDN1 (endothelin-1 precursor; LFC= 2.11) and two glucose transporters SLC2A1 (GLUT1; LFC= 2.552) and SLC2A14 (GLUT14; LFC= 3.555) (FIG 5/D). Interestingly, an overlap could also be observed among the applied conditions in terms of the expression of specific target genes, but without the targeting miRNAs. This suggests, that under the different conditions, the expression of the examined genes is possibly regulated by other post- transcriptional regulatory processes.

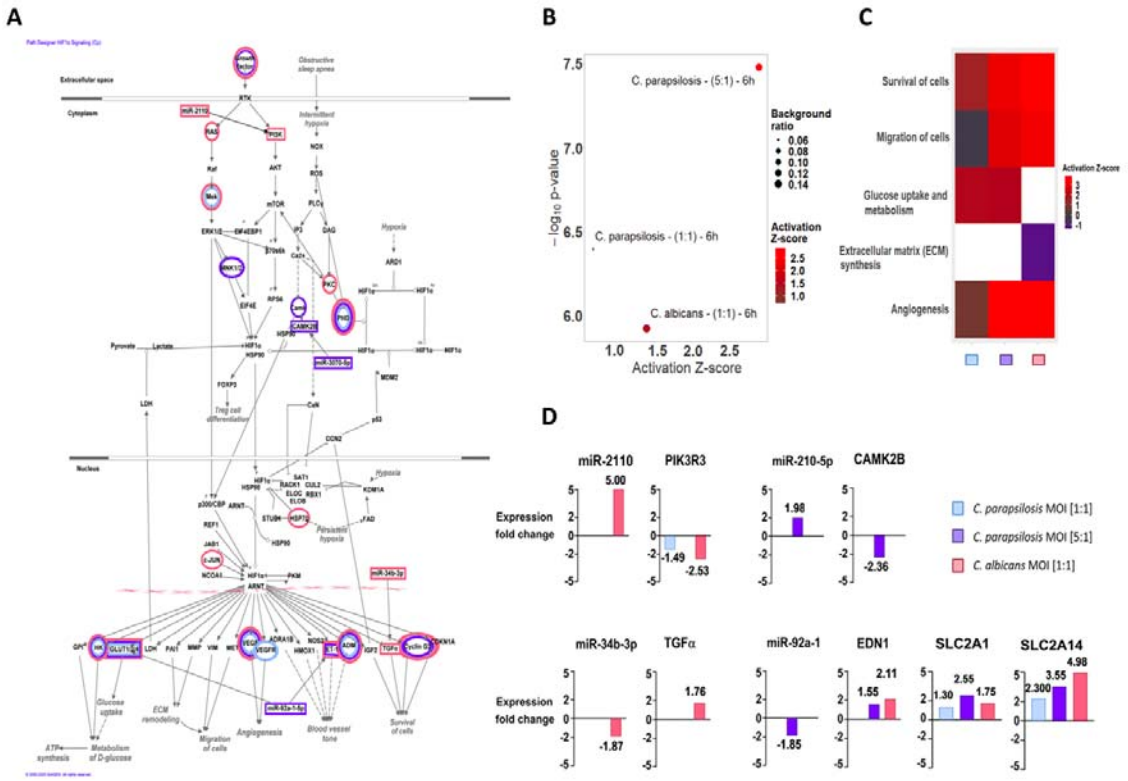

FIG 5 -Results of the IPA analyses on HIF1-α signaling-related molecular components and functions. (A) Significantly down- or overexpressed genes in each condition were visualized within the canonical HIF1-α signal transduction network using pathway explorer and designer tools within IPA. The individual genes affected by each treatment were marked by the corresponding colors of each condition: blue: *C. parapsilosis* MOI 1:1, purple: MOI 5:1 and red: *C. albicans* MOI 1:1. (B) The significance of the pathway activation and direction were determined by the p-value of overlap (<0.05) after performing an expression core analysis in IPA on the set of DEGs in each applied condition. (C) The direction of activation of the functions regulated by this signaling pathway was analyzed similarly, the blank rectangles (white) mean that we could not observe a significant regulation of that particular biological function under after the corresponding treatment. (D) We selected the miRNA-mRNA target pairs involved in this signaling pathway after applying several filtering steps in IPA's miRNA target filter tools. We only considered pairs that showed significant, opposite regulation in

corresponding treatments, in which the targets were scientifically proven to be involved in HIF1-α signaling and the target site on the mRNA was either experimentally proven or strongly predicted by IPA based on base complementarity.

Hepatic-fibrosis / stellate cell (HSC) activation-pathway discriminates between the strong and attenuated inflammatory response towards the two species

The other signaling pathway that was simultaneously regulated by all three conditions after 6 hours was the hepatic fibrosis or hepatic stellate cell (HSC) pathway - a pathway involved in stellate cell activation during hepatic inflammation and injury. The early signaling events during the activation of HSCs and in activated HSCs are shown on FIG 6/A. Similar to the HIF1- α pathway, several genes showed either species-specific or treatment-influenced expression changes (FIG 6/A). The regulation of the signal transduction pathway by *C. parapsilosis* MOI 1: 1 and 5: 1 and *C. albicans* MOI 1: 1 was also statistically significant, although the direction of change could not be determined, due to the incoherent changes in gene expression (FIG 6/B). This pathway is associated with a number of biological functions related to inflammation, cellular activation, chemotaxis, apoptotic cell death or tumor cell proliferation. In general, *C. albicans* stimuli led to the overall activation of proinflammatory responses (e.g. upregulation of chemotaxis, cellular activation), while *C. parapsilosis* treatment resulted in either only a mild inflammatory response (e.g. immune cell activation with MOI 5:1), or no significant effect (chemotaxis and cellular activation with MOI 1:1; and inflammation and chemotaxis response for MOI 5:1) (FIG 6/C). Host cell apoptosis was inhibited by all three applied fungal conditions, although *C. parapsilosis* MOI 1:1 elicited the strongest inhibitory effect (z-score = -2.059). Interestingly, contrarily to the robust host tumor cell proliferation promoting effect of both *C. albicans* and *C. parapsilosis* MOI 5:1, the low dose application of *C. parapsilosis* led to a mild inhibitory effect (z-score = 2.260, 2.248 and -0.586, respectively) (FIG 6/C).

Similar to the HIF1- α pathway, miRNA-mRNA target pairs could be identified after C. *albicans* and *C. parapsilosis* MOI 5: 1 stimulus, but not after the lower *C. parapsilosis* infection dose. Four miRNAs with altered expression were identified in *C. albicans* treated cells, namely miR-2110 (LFC= 5.00), miR-4485 (LFC= -2.19), miR-34b (LFC= -1.87), miR-4677 (LFC= -1.73), and their potential counterparts included IGFBP5 (insulin-like growth factor-binding protein 5; LFC= -3.81), KLF6 (kruppel-like factor 6; LFC= 1.58), TGF-α (LFC= 1.76), and IL-8 (chemokine; LFC= 9.90), respectively (Figure 6/D). After *C.*

372 *parapsilosis* MOI 5:1 treatment, miR-92a and its potential target (EDN1) as well as miR-543
373 (LFC= -3.38) and its potential target IGFBP3 (insulin-like growth factor-binding protein 3;
374 LFC= 4.20) were identified. Although no regulatory miRNAs were identified after *C.*
375 *parapsilosis* MOI 1:1 treatment, we found altered expressions of KLF6 and IGFBP5,
376 suggesting that they were possibly regulated by other post- transcriptional regulatory
377 processes.
378 In this pathway, each of the targeted genes primarily affect inflammatory functions. Thus, the
379 miRNA silencing observed here may contribute to the discrimination of the inflammatory
380 response to *C. albicans* and *C. parapsilosis.*

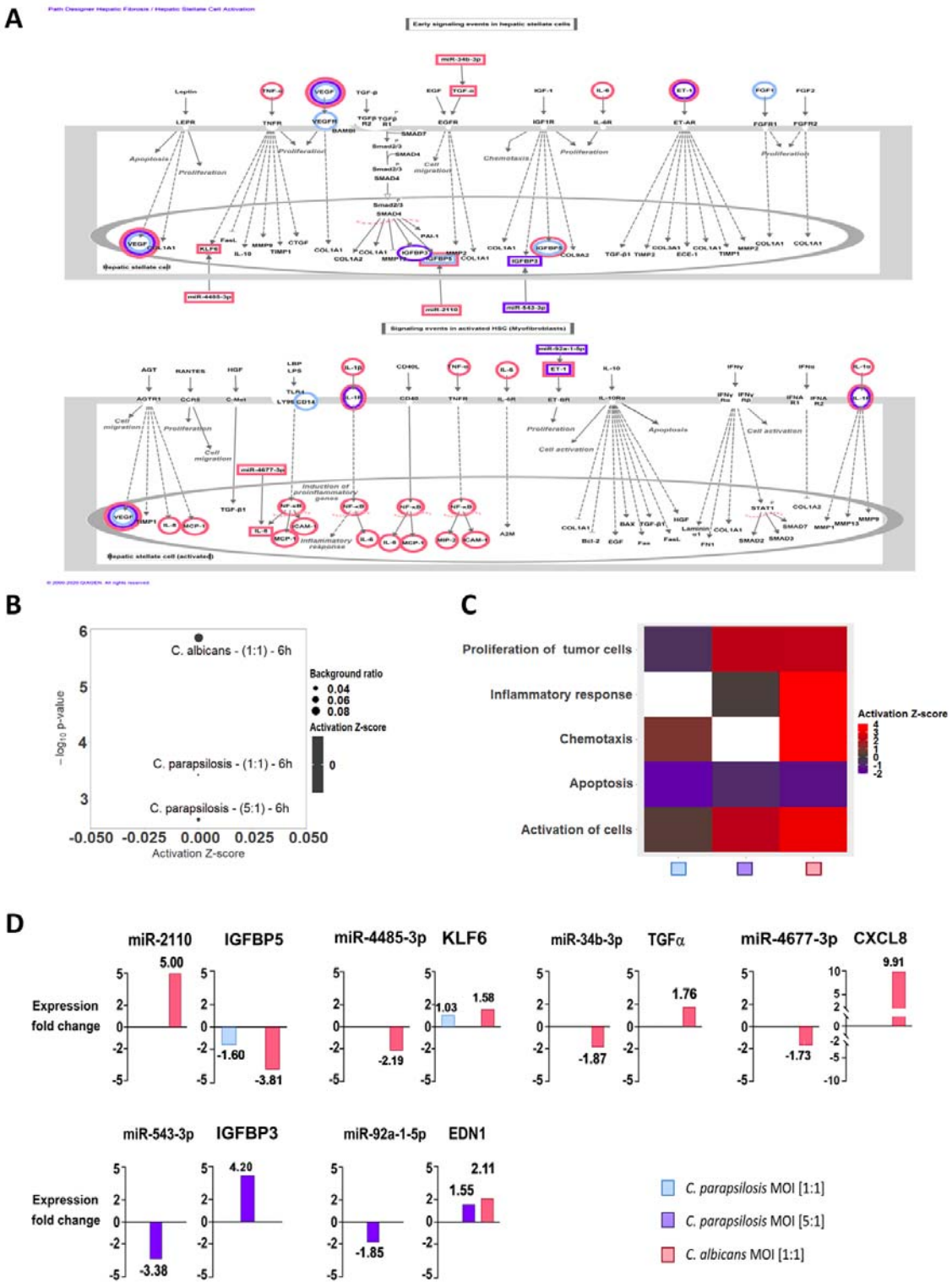

FIG 6 - Results of the IPA analyses of Hepatic-fibrosis/stellate cell activation signaling. (A) Similar to the HIF1-α signal transduction network, regulated molecular components were visualized via pathway designer tools; (B) direction of activation of the hepatic-fibrosis signaling related functions were analyzed after an

385 expression core analysis of the DEGs; (C) pathway activation was also examined and (D) miRNA-miRNA-
386 targets were analyzed via miRNA target filter tools under similar conditions.

387

Discussion

In this study, we aimed to dissect and compare host responses triggered by *C. albicans* and C. *parapsilosis* - two common fungal residents of the oral microbial community - in oral ECs derived from a healthy individual (34). Our findings indicate that the EC immune response actively discriminates between *C. albicans* and *C. parapsilosis*, as shown by the significant differences in host LDH release, chemokine, cytokine and antimicrobial peptide responses. In our model, *C. parapsilosis* failed to evoke a robust, immediate proinflammatory response compared to *C. albicans*, which is similar to what has been observed in other experimental infection models (35–39). These findings are also comparable with earlier studies of *Candida* - EC interactions, showing that only *C. albicans* triggers a strong inflammatory response during the colonization of the oral epithelial barrier (36). To aid the understanding of how oral ECs might discriminate between the two species and thus distinguish a species with a higher pathogenic potential from one that more commonly is a mucosal commensal, we examined host cell transcriptomic changes following yeast-EC interaction.

Our findings revealed significant differences in host cell transcriptomic responses that were species-specific. With *C. albicans* co-culture, the majority of signaling routes and pathways were specific to the inflammatory response, and resulted in the activation of e.g. NF-κB and IL-17 signaling pathways (both are required for epithelium protection during oral candidiasis), which is in line with previous reports (40–42). *C. parapsilosis* challenge, however, led to the activation of various, mainly inflammation-independent pathways, such as carbohydrate metabolism-, hypoxia- and cardiovascular development -related responses, and, interestingly, pathways frequently associated with carcinogenesis, none of which have been previously associated with this species. Glucose homeostasis maintenance has recently been suggested to be required for efficient anti-*C. albicans* immune responses (43). According to Tucey et al., *C. albicans* depletes glucose from human and murine macrophages during infection, thereby accelerating host cell death. Although no studies are available comparing the carbon metabolism of *C. albicans* and *C. parapsilosis*, high glucose tolerance and rapid proliferation of *C. parapsilosis* in glucose rich parenteral nutrition has previously been reported (44–46). This suggests enhanced glucose metabolic processes in this species, and also that during *C. parapsilosis* infections regulation of host glucose metabolism, as a virulence factor, might be even more momentous. Although further research is required to confirm this hypothesis, considering that the highest risk group of *C. parapsilosis* infections includes low-birth weight neonates (47), the population primarily receiving parenteral

nutrition, interfering with the pathogen's carbon metabolic processes might reduce the risk of invasive candidiasis development in this patient group. Damaged tissues and inflammation are often coupled with local hypoxia (48). The lack of severe host cell damage and proinflammatory responses upon high-dose *C. parapsilosis* challenge, suggests that the significantly altered hypoxic responses have other origins. Such responses could arise simply due to the elevated fungal burden rapidly depleting available oxygen levels through the rapid outgrowth of host cells. Host responses related to cardiovascular development and the activation of pathways frequently associated with carcinogenesis during *C. parapsilosis* treatment are also unique. No such phenomenon has been previously associated with this species. Such novel information sets the ground for a new aspect of future experimental investigations in the field of *Candida* research together with cancer biology.

Besides the species-specific activated pathways, signaling pathways with simultaneous regulation by all three conditions were also found. Even among these, condition-specific transcriptional responses could be identified. One such pathway was hypoxia inducible factor 1-α (HIF-1α) signaling. HIFs, especially HIF-1α, have previously been demonstrated to regulate various innate immune processes (49). Although a study showed that HIF-1α activation by β-glucan and commensal bacteria promotes protection against subsequent *C. albicans* infections *in vivo* (50,51), suggesting the pathway's inclusion in anti-*Candida* responses, little is known about its role in antifungal immunity regulation. Our results suggest that activation of the HIF-1α pathway is divergent. While *C. albicans* stimulus promoted signaling processes related to cell survival and migration, or inhibition of ECM synthesis, glucose uptake and metabolism-related processes dominated after *C. parapsilosis* co-culture. While regulation of EC protective cellular responses seems to be a priority in the case of *C. albicans,* in line with previous reports (52), regulation of carbohydrate metabolism appears to be a unique characteristic of *C. parapsilosis* stimulus. In the HSC-activation pathway, the other pathway simultaneously activated by all conditions, both species regulated signaling processes primarily involved in inflammation. Although *C. albicans* challenge resulted in the overall activation of proinflammatory responses, *C. parapsilosis* co-culture led to only a mild effect. Species-specific regulation of both HIF-1α signaling and the HSC-activation pathway might be what determines the outcome of the triggered innate immune responses of oral ECs.

Subsequent miRNA analyses revealed condition-specific posttranscriptional regulation of the transcriptomic responses. Among the identified dysregulated miRNA-species, 4 were associated with co-culturing EC with *C. parapsilosis* MOI 1:1, 10 with MOI 5:1 and 18 with *C. albicans*. Among the miRNAs identified during *C. albicans* treatment, only miRNA-16-1p

has been previously associated with *C. albicans* infections (28). Out of the remaining 17 differentially expressed miRNAs, miR-20a and hsa-let-7 have been reported to regulate anti-fungal responses, although only in *P. brasiliensis* (53). miR-16 and miR-4677 have been linked to antibacterial host responses (54,55), while miR-3074, miR-335, miR-34b, miR-4485 and miR-1246 have been associated with antiviral immune responses in various *in vitro* models (56–60). The remaining 9 identified miRNA species have not yet been associated with microbe-induced inflammatory responses. In contrast, except for miR-3064 and miR-1294, all of the miRNAs differentially regulated in the presence of *C. parapsilosis* have been suggested to regulate host responses during microbial stimuli. miR-210 was previously associated with *C. albicans* (26), miR-125b with *P. brasiliensis* (61), and miR-92a with *P. americana* infections (62). Other than antifungal host responses, miR-4755 and miR-4677 deregulation was previously linked to bacterial stimuli (55,63), miR-1305, miR-627, miR-543 and miR-581 to viral challenge, and miR-12135 to parasitic infections (64). miR-1277 and miR-365 were associated with host responses upon both bacterial and viral infections (65–69). Thus, although less miRNA species could be coupled with *C. parapsilosis* infections than with *C. albicans*, the majority of these were confirmed regulators of anti-microbial responses. It is noteworthy that several of the miRNAs identified after both *C. albicans* and *C. parapsilosis* stimuli have also been associated with various tumorigenic processes (70–75), further highlighting that fungal colonization might actively influence tumorigenic processes, as suggested previously (76,77).

Subsequent analyses revealed that the yeast-specifically identified miRNA-species regulate the expression of genes involved in condition-specific activated pathways, including survival, proliferation and inflammation in *C. albicans* and vascular development and carbohydrate metabolism-related pathways in *C. parapsilosis* co-cultures. For instance, miR-92a was identified in HIF1-α signaling, potentially regulating the expression of GLUT1 (SLC2A1) and GLUT14 (SLC2A14), two glucose transporters required for carbohydrate metabolism maintenance (78) as well as the expression of EDN1 (endothelin-1) (79), a potent vasoconstrictor, during *C. parapsilosis* infection. The finding that both GLUT1 and GLUT14 are also upregulated upon *C. albicans* stimulus suggests, that the significant activation of carbohydrate metabolic processes by *C. parapsilosis* is the result of an additive effect and glucose metabolic regulators, other than the mentioned glucose transporters, are also deregulated during the stimulus. In the same pathway, following *C. albicans* challenge, miR-34b was linked to TGF-α expression, a known regulator of survival and cell proliferation after its activation by hypoxia-induced factors (such as HIF1-α) (80), and miR-2110 was found to

repress PIK3R3 expression, a subunit of PI3K, thereby interfering with proinflammatory responses (81,82).

In the HSC-activation pathway, besides miR-92a and its target EDN-1, miR-543 was also identified, which targets IGFBP3, an IGF binding protein previously linked to apoptosis regulatory processes (83). Although independent of IGFBP3 expression changes, apoptosis inhibition as a potential outcome of HSC-activation was predicted to be the strongest following the low-dose *C. parapsilosis* treatment. With *C. albicans* infection, besides the abovementioned miR-34b - TGF-α pair, miR-2110 was identified as a potential regulator of IGFBP5, miR-4485 was linked to KLF6 regulation and miR-467 to regulating CXCL8 expression. KLF6 is a zinc finger transcription factor previously reported to promote inflammation in macrophages (84). IGFBP5, another IGF binding protein, was reported to be a potent chemoattractant of immune cells (85). CXCL8 is a well-known chemokine secreted by oral ECs upon *C. albicans* stimuli (86), in line with our data. Thus, all three miRNA target genes are potential inflammation regulatory components of the anti-*C. albicans* oral EC response.

Taken together, the in-depth analyses of the two simultaneously, yet diversely regulated signaling pathways also support the major, species-specific findings of the transcriptome functional analyses, and suggest that the differentiating EC responses might indeed derive from altered posttranscriptional regulations. Although the obtained results shed some light on the potential underlying molecular mechanisms enabling species-specific host responses, further investigations and experimental studies are required to support these findings.

In summary, we can conclude that human oral ECs are able to actively differentiate between *Candida* species through altered posttranscriptional regulatory processes. (FIG 7). While the presence of *C. parapsilosis* stimulus does not generate a robust inflammatory response in ECs, an elevated fungal burden can initiate inflammatory responses, albeit in a much less rapid and robust manner compared to *C. albicans*. Additionally, we found that different fungal burdens of *C. parapsilosis* led to the variable induction of generic alterations with the higher MOI inducing a broader and more significant response. The species-specific fine tuning of both HIF-1α signaling and HSC-activation pathways via miRNA silencing could also be a key to the distinct epithelial responses. The *in silico* data acquired through this project aid our current understanding of how healthy oral ECs might discriminate between *Candida* species with high or low pathogenic potential in the human oral mucosa.

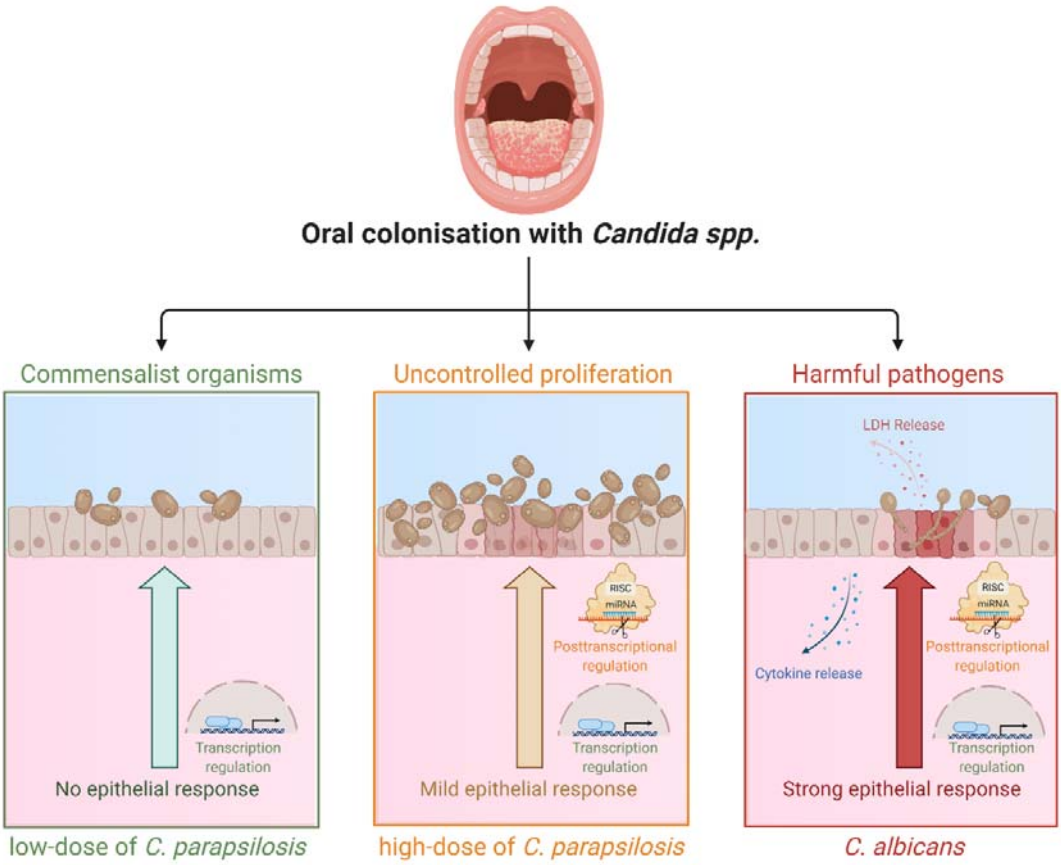

FIG 7 - Altered innate immune response regulation in healthy oral ECs discriminate between low-dose *C. parapsilosis*, increased dose of *C. parapsilosis* and *C. albicans* stimuli.

Materials and Methods

Strains and growth conditions

In this study, *C. parapsilosis* CLIB 214 and *C. albicans* SC5314 laboratory strains were used. *Candida* strains were maintained on solid penicillin/streptomycin-supplemented YPD medium at 4°C. Prior to host cell stimulation, yeast cells were grown overnight at 30°C in liquid YPD medium, washed 3x with phosphate-buffered saline (PBS) and counted using a haemocytometer to adjust the desired cell concentration.

Stimulation of OKF6/TERT2 cells

The oral EC line OKF6/TERT2, a telomerase deficient EC line derived from a healthy individual, was used for all experiments and maintained as described previously (34). Oral ECs were then plated in 6-well plates in keratinocyte serum-free medium (K-SFM) supplemented with 25 µg/ml BPE, 2 ng/ml rEGF, 2mM L-Glutamine and 0.5% penicillin-streptomycin and cells were grown to 90% confluency. OKF6/TERT2 cells were then stimulated with *C. parapsilosis* and *C. albicans* in serum-free K-SFM medium. Depending on the experiment, either cell free supernatants or host cells were collected following fungal exposure and stored at -80°C or used immediately.

Lactate dehydrogenase assay

Host cell damage by *C. albicans* and *C. parapsilosis* was determined by LDH cytotoxicity detection kit according to the manufacturer's instructions. OKF6/TERT2 cells were challenged with fungal cells at MOIs of 1:5, 1:2, 1:1, 2:1 and 5:1 or left untreated at various time points. During analysis, the values corresponding to the levels of LDH activity measured in untreated samples were subtracted from the values of stimulated samples. The percentage of cytotoxicity was determined as (OD experimental value/OD positive control)□×□100. 1% Triton X-100 treated samples served as positive controls. Results are derived from 3 triplicate experiments.

Total RNA and miRNA extraction

Total RNA and miRNA extraction from OKF6/TERT2 cells were carried out with miRNeasy Mini Kits according to the manufacturer's instructions, allowing for the simultaneous extraction of total RNA and miRNA. Cells were grown until 90% confluency in tissue culturing 6-well-plates in supplemented K-SFM medium, washed once with PBS, and stimulated with *C. albicans* (MOI of 1:1) or *C. parapsilosis* (MOI of 1:1 and/or 5:1) in

unsupplemented K-SFM medium. Following co-incubation, host cells were washed 2x with PBS and treated with the supplied TRIzol lysis reagent. After host cell lysis, phase separation and purification of RNA (both total and miRNA), we performed quantity and quality checks of the samples before proceeding to cDNA library preparation or cDNA synthesis and subsequent sequencing. Three independently treated biological parallels were used.

cDNA synthesis and real-time PCR analysis

For preliminary expression studies, 1000 ng of RNA was utilized for cDNA synthesis using the RevertAid first strand cDNA synthesis kit. Primers for qPCR analyses are listed in Table S1. The amplification conditions were as follows: one cycle of denaturation for 3 min at 95°C; denaturation at 95°C for 10 s; 49 cycles of annealing at 60°C for 30 s, and elongation at 65°C for 30 s; with a final extension step at 72°C for 30 s. β2-microglobulin was used as an internal control. Relative normalized expression values (unstimulated host cells served as controls) were calculated and presented.

Sequencing library preparation and RNA-sequencing

miRNA sequencing libraries were prepared using NEBNext Multiplex Small RNA Library Prep Set for Illumina following the manufacturer's protocol. Libraries were size selected using AMPure XP beads and after validation with an Agilent 2100 Bioanalyzer instrument sequenced with an Illumina MiSeq DNA sequencer using Illumina MiSeq Reagent kit V3-150.

Transcriptome analysis

We performed the preliminary quality analysis and trimming using FastQC and Cutadapt command line tools on the raw sequence files. Next, we fit the reads to the reference genome index (GRCh38) using HISAT2 (88), with the parameters --dta --non-deterministic --rna-strandness. Read numbers were calculated using the GenomicAlignments package, and differential gene expression in logarithmic fold change (LFC) was then performed using the DeSeq2 tool (89). We filtered out objects with read counts lower than 1 part per million (ppm). In the experimentally derived gene list, differentially expressed genes (DEGs) were counted above the absolute value of the logarithmic fold change > 1.5 and the adjusted p-value < 0.05.

Short-read mapping and counting

The sequenced reads were mapped to known microRNA precursors, and novel sequences downloaded from miRBase (version 22) using miRDeep2.0 (90). Hits with a read count below 1 ppm were filtered out from further analysis. The distorting effect caused by the hits that were expressed at an exceptionally high level (and have the largest variance) was corrected via DeSeq2, and the p-value corrected by null distribution using the fdrtool package. The cut-off values for the significant hits were set at a p-value < 0.05 and the absolute value of the logarithmic fold change > 1.5.

Overrepresentation analyses

Upon completion of the genome-wide RNA and miRNA expression analyses, gene expression data was interpreted using overrepresentation analyses (ORA) and gene-set enrichment analyses (GSEA) provided in the Bioconductor package, DOSE (91) and clusterProfiler (92) (FIG 3/A). The two ORAs - KEGG over-representation test and GO over-representation test - as well as the GO GSEA were carried out, against a constant background, for which purpose, the human genome wide annotation package ('org.Hs.eg.db') was used (93). During both analyses the most robust Benjamini & Hochberg (1995) ("BH") method was used for the multiple comparison p-value adjustment, and pathways $p < 0.05$ were considered significantly overrepresented. The enrichment results were visualized as dotplots via the enrichplot package. For further data mining, we calculated the semantic similarity (SS) of the found GO terms to establish connections between genes targeted by a specific miRNA via the ViSEAGO package (https://doi.org/10.1186/s13040-019-0204-1). These results were visualized on a multidimensional scaling plot (MDS) that represents the distance among the set of enriched GO terms on the first two dimensions, which highlight possible clustering patterns.

Causal analyses

We employed causal analysis methods included in the Qiagen licensed, leading-edge bioinformatical software Ingenuity Pathway Analysis (IPA) and we ran expression core analyses on our samples. Among the included algorithms, we used downstream Effect Analysis (DEA) to observe each treatment's effect on the biological functions of the host cells. Furthermore, we concluded miRNA-target analyses to find possible miRNA-mRNA target pairs with significant, anti-correlated expression. We employed the p-value of overlap and the activation Z-score to determine the significance of the prediction in IPA, which are

the two most important parameters to achieve this (94). The p-value of overlap determines the statistical significance based on the overlap of the observed and predicted regulated gene sets, while the activation Z-score predicts the direction of regulation depending on the parallelism in the observed and predicted over / down-regulatory patterns. In our experiments, only the predictions with p-value <0.05 were considered significant hits. We further specified that only experimentally proven or strongly predicted intermolecular relationships should be considered.

Statistical analysis

All statistical analyses were performed with GraphPad Prism v 6.0 software using parametric *t* tests or nonparametric Mann-Whitney tests. The values for the groups examined were considered statistically significantly different at $p < 0.05$.

Data availability

Data upload is in progress. Further data are available upon request from the corresponding author.

Competing interests

The authors declare no conflict of interest.

Acknowledgements

MH and this research work was supported by the Szeged Scientists Academy under the sponsorship of the Hungarian Ministry of Innovation and Technology (FEIF/433-4/2020-ITM_SZERZ). This work was supported by grants 20391-3/2018/FEKUSTRAT, NKFIH K 123952, and GINOP-2.3.2.-15-2016-00015. A.G. was further funded by LP2018-15/2018.
This study was also supported by the Hungarian National Research, Development and Innovation Office (NKFIH) grant GINOP-2.3.2-15-2016-00035.
László Bodai was supported by the ÚNKP-20-5-SZTE-642 New National Excellence Program of the Ministry for Innovation and Technology and by the János Bolyai Research Scholarship (BO/00522/19/8) of the Hungarian Academy of Sciences.

Author contributions:

AG and RT contributed to the concept and design of this project. MH and RT carried out the majority of experiments with the help of GN, NZs, CsV, JDN. MH and GN, LB, PH analyzed the aquired data. MH prepared the manuscript and the figures, that was revised by R.T. with A.G. All authors reviewed the manuscript, contributed to the discussion and approved the final version.

665

Supplementary Tables

Table S1 - List of primers used for qPCR analyses.

Table S2 - Identified differentially expressed genes (DEGs) following fungal stimuli.

Table S3 - List of miRNA-specific target mRNAs identified following *C. parapsilosis* MOI 1:1 stimulus.

Table S4 - List of miRNA-specific target mRNAs identified following *C. parapsilosis* MOI 5:1 stimulus.

Table S5 - List of miRNA-specific target mRNAs identified following *C. albicans* MOI 1:1 stimulus.

Table S6 - KEGG analysis results of *C. albicans* MOI 1:1 stimulus after 6 hours.

Table S7 - GO term analysis results of *C. albicans* MOI 1:1 stimulus after 6 hours.

Table S8 - KEGG analysis results of *C. parapsilosis* MOI 1:1 stimulus after 6 hours.

Table S9 - GO term analysis results of *C. parapsilosis* MOI 1:1 stimulus after 6 hours.

Table S10 - KEGG analysis results of *C. parapsilosis* MOI 5:1 stimulus after 6 hours.

Table S11 - GO term analysis results of *C. parapsilosis* MOI 5:1 stimulus after 6 hours.

Table S12 - GO term analysis results of miRNA-specific target mRNAs identified following *C. albicans* MOI 1:1 stimulus.

Table S13 - GO term analysis results of miRNA-specific target mRNAs identified following *C. parapsilosis* MOI 5:1 stimulus.

References

1. Avila PC, Schleimer RP. Airway epithelium. In: Allergy and Allergic Diseases, Second Edition. Wiley-Blackwell; 2009. p. 366–97.
2. Schleimer RP, Kato A, Kern R, Kuperman D, Avila PC. Epithelium: At the interface of innate and adaptive immune responses. Vol. 120, Journal of Allergy and Clinical Immunology. 2007.
3. Calderone RA, Clancy CJ. Candida and candidiasis. American Society for Microbiology Press; 2011.
4. Vázquez-González D, Perusquía-Ortiz AM, Hundeiker M, Bonifaz A. Opportunistic yeast infections: Candidiasis, cryptococcosis, trichosporonosis and geotrichosis. JDDG - J Ger Soc Dermatology. 2013;11(5).
5. Pappas PG, Lionakis MS, Arendrup MC, Ostrosky-Zeichner L, Kullberg BJ. Invasive candidiasis. Nat Rev Dis Prim. 2018;4(1):18026.
6. Sobel JD. The emergence of non-albicans Candida species as causes of invasive candidiasis and candidemia. Vol. 8, Current Infectious Disease Reports. 2006. p. 427–33.
7. Manolakaki D, Velmahos GC, Kourkoumpetis T, Chang Y, Alam HB, De Moya MM, et al. Candida infection and colonization among trauma patients. Virulence. 2010;
8. Ghannoum MA, Jurevic RJ, Mukherjee PK, Cui F, Sikaroodi M, Naqvi A, et al. Characterization of the oral fungal microbiome (mycobiome) in healthy individuals. PLoS Pathog. 2010 Jan;6(1).
9. Peters BA, Wu J, Hayes RB, Ahn J. The oral fungal mycobiome: Characteristics and relation to periodontitis in a pilot study. BMC Microbiol. 2017;
10. Berkovits C, Toth A, Szenzenstein J, Deak T, Urban E, Gacser A, et al. Analysis of oral yeast microflora in patients with oral squamous cell carcinoma. Springerplus. 2016/08/19. 2016;5(1):1257.
11. Olivas-Escárcega V, Ruiz-Rodríguez MDS, Fonseca-Leal MDP, Santos-Díaz MÁ, Gordillo-Moscoso A, Hernández-Sierra JF, et al. Prevalence of oral candidiasis in chronic renal failure and renal transplant pediatric patients. J Clin Pediatr Dent. 2008;32(4).
12. Abu-Elteen KH, Hamad MA, Salah SA. Prevalence of oral candida infections in diabetic patients. Bahrain Med Bull. 2006;28(1).
13. Singh GK, Capoor MR, Nair D, Bhowmik KT. Spectrum of fungal infection in head

and neck cancer patients on chemoradiotherapy. J Egypt Natl Canc Inst. 2017;29(1).

14. Gaitán-Cepeda LA, Sánchez-Vargas O, Castillo N. Prevalence of oral candidiasis in HIV/AIDS children in highly active antiretroviral therapy era. A literature analysis. Vol. 26, International Journal of STD and AIDS. 2015.

15. Almeida RS, Brunke S, Albrecht A, Thewes S, Laue M, Edwards JE, et al. The hyphal-associated adhesin and invasin Als3 of Candida albicans mediates iron acquisition from host ferritin. PLoS Pathog. 2008;

16. Noble SM, Gianetti BA, Witchley JN. Candida albicans cell-type switching and functional plasticity in the mammalian host. Nature Reviews Microbiology. 2017.

17. Moyes DL, Wilson D, Richardson JP, Mogavero S, Tang SX, Wernecke J, et al. Candidalysin is a fungal peptide toxin critical for mucosal infection. Nature. 2016;

18. Moyes DL, Runglall M, Murciano C, Shen C, Nayar D, Thavaraj S, et al. A biphasic innate immune MAPK response discriminates between the yeast and hyphal forms of Candida albicans in epithelial cells. Cell Host Microbe. 2010/09/14. 2010;8(3):225–35.

19. Tóth R, Nosek J, Mora-Montes HM, Gabaldon T, Bliss JM, Nosanchuk JD, et al. Candida parapsilosis: From genes to the bedside. Clinical Microbiology Reviews. 2019.

20. Rippon JW. Medical mycology; the pathogenic fungi and the pathogenic actinomycetes. Eastbourne, UK; WB Saunders Company; 1982.

21. Dismukes WE, Pappas PG, Sobel JD. Clinical mycology. Oxford University press, USA; 2003.

22. Tata W, Thepbundit V, Kuansuwan C, Preechasuth K. Distribution of Candida species in oral candidiasis patients: Association between sites of isolation, ability to form biofilm, and susceptibility to antifungal drugs. 2019 Jan 1;1–7.

23. Jayachandran AL, Katragadda R, Thyagarajan R, Vajravelu L, Manikesi S, Kaliappan S, et al. Oral Candidiasis among Cancer Patients Attending a Tertiary Care Hospital in Chennai, South India: An Evaluation of Clinicomycological Association and Antifungal Susceptibility Pattern. Can J Infect Dis Med Microbiol. 2016;2016:8758461.

24. Nahid MA, Satoh M, Chan EKL. MicroRNA in TLR signaling and endotoxin tolerance. Vol. 8, Cellular and Molecular Immunology. 2011.

25. Nahid MA, Satoh M, Chan EKL. Interleukin 1β-Responsive MicroRNA-146a Is Critical for the Cytokine-Induced Tolerance and Cross-Tolerance to Toll-Like Receptor Ligands. J Innate Immun. 2015;7(4).

26. Du L, Chen X, Duan Z, Liu C, Zeng R, Chen Q, et al. MiR-146a negatively regulates dectin-1-induced inflammatory responses. Oncotarget. 2017;8(23).
27. Monk CE, Hutvagner G, Arthur JSC. Regulation of miRNA transcription in macrophages in response to candida albicans. PLoS One. 2010;
28. Muhammad SA, Fatima N, Syed NIH, Wu X, Yang XF, Chen JY. MicroRNA expression profiling of human respiratory epithelium affected by invasive candida infection. PLoS One. 2015;10(8).
29. Khurshid Z, Naseem M, Sheikh Z, Najeeb S, Shahab S, Zafar MS. Oral antimicrobial peptides: Types and role in the oral cavity. Vol. 24, Saudi Pharmaceutical Journal. 2016.
30. Bals R. Epithelial antimicrobial peptides in host defense against infection. Vol. 1, Respiratory Research. 2000.
31. Németh T, Tóth A, Szenzenstein J, Horváth P, Nosanchuk JD, Grózer Z, et al. Characterization of Virulence Properties in the C. parapsilosis Sensu Lato Species. PLoS One. 2013;8(7).
32. Horváth P, Nosanchuk JD, Hamari Z, Vágvölgyi C, Gácser A. The identification of gene duplication and the role of secreted aspartyl proteinase 1 in Candida parapsilosis virulence. J Infect Dis. 2012;205(6).
33. Tóth A, Németh T, Csonka K, Horváth P, Vágvölgyi C, Vizler C, et al. Secreted Candida parapsilosis lipase modulates the immune response of primary human macrophages. Virulence. 2014;5(4).
34. Hahn WC, Ino Y, Ronfard V, Wu JYd, Weinberg R a, Louis DN, et al. Human keratinocytes that express hTERT and also bypass a p16(INK4a)-enforced mechanism that limits life span become immortal yet retain normal growth and differentiation characteristics. Mol Cell Biol. 2000;20(4).
35. Toth A, Csonka K, Jacobs C, Vagvolgyi C, Nosanchuk JD, Netea MG, et al. Candida albicans and Candida parapsilosis induce different T-cell responses in human peripheral blood mononuclear cells. J Infect Dis. 2013/05/11. 2013;208(4):690–8.
36. Moyes DL, Murciano C, Runglall M, Kohli A, Islam A, Naglik JR. Activation of MAPK/c-Fos induced responses in oral epithelial cells is specific to Candida albicans and Candida dubliniensis hyphae. Med Microbiol Immunol. 2011/06/28. 2012;201(1):93–101.
37. Villar CC, Kashleva H, Mitchell AP, Dongari-Bagtzoglou A. Invasive phenotype of Candida albicans affects the host proinflammatory response to infection. Infect Immun.

2005;73(8).

38. Weindl G, Naglik JR, Kaesler S, Biedermann T, Hube B, Korting HC, et al. Human epithelial cells establish direct antifungal defense through TLR4-mediated signaling. J Clin Invest. 2007/11/10. 2007;117(12):3664–72.

39. Hirayama T, Miyazaki T, Ito Y, Wakayama M, Shibuya K, Yamashita K, et al. Virulence assessment of six major pathogenic Candida species in the mouse model of invasive candidiasis caused by fungal translocation. Sci Rep. 2020;10(1).

40. Mengesha BG, Conti HR. The role of IL-17 in protection against mucosal Candida infections. Vol. 3, Journal of Fungi. 2017.

41. Verma AH, Richardson JP, Zhou C, Coleman BM, Moyes DL, Ho J, et al. Oral epithelial cells orchestrate innate type 17 responses to Candida albicans through the virulence factor candidalysin. Sci Immunol. 2017;2(17).

42. Naglik JR, König A, Hube B, Gaffen SL. Candida albicans–epithelial interactions and induction of mucosal innate immunity. Vol. 40, Current Opinion in Microbiology. 2017.

43. Tucey TM, Verma J, Harrison PF, Snelgrove SL, Lo TL, Scherer AK, et al. Glucose Homeostasis Is Important for Immune Cell Viability during Candida Challenge and Host Survival of Systemic Fungal Infection. Cell Metab. 2018;27(5).

44. Trofa D, Gácser A, Nosanchuk JD. Candida parapsilosis, an Emerging Fungal Pathogen. Clin Microbiol Rev. 2008 Oct;21(4):606–25.

45. Pereira L, Silva S, Ribeiro B, Henriques M, Azeredo J. Influence of glucose concentration on the structure and quantity of biofilms formed by Candida parapsilosis. FEMS Yeast Res. 2015;15(5).

46. Solomon SL, Khabbaz RF, Parker RH, Anderson RL, Geraghty MA, Furman RM, et al. An Outbreak of Candida parapsilosis Bloodstream Infections in Patients Receiving Parenteral Nutrition. J Infect Dis. 1984 Jan 1;149(1):98–102.

47. Pammi M, Holland L, Butler G, Gacser A, Bliss JM. Candida parapsilosis is a significant neonatal pathogen a systematic review and meta-analysis. Pediatr Infect Dis J. 2013;32(5).

48. Krzywinska E, Stockmann C. Hypoxia, metabolism and immune cell function. Vol. 6, Biomedicines. 2018.

49. Zinkernagel AS, Johnson RS, Nizet V. Hypoxia inducible factor (HIF) function in innate immunity and infection. Vol. 85, Journal of Molecular Medicine. 2007.

50. Esher SK, Fidel PL, Noverr MC. Candida/staphylococcal polymicrobial intra-

abdominal infection: pathogenesis and perspectives for a novel form of trained innate immunity. Vol. 5, Journal of Fungi. 2019.

51. Cheng S-C, Quintin J, Cramer RA, Shepardson KM, Saeed S, Kumar V, et al. mTOR- and HIF-1α–mediated aerobic glycolysis as metabolic basis for trained immunity. Science (80-). 2014;345(6204).

52. Muñoz JF, Delorey T, Ford CB, Li BY, Thompson DA, Rao RP, et al. Coordinated host-pathogen transcriptional dynamics revealed using sorted subpopulations and single macrophages infected with Candida albicans. Nat Commun. 2019;10(1).

53. Marioto DTG, Dos Santos Ferraro ACN, De Andrade FG, Oliveira MB, Itano EN, Petrofeza S, et al. Study of differential expression of miRNAs in lung tissue of mice submitted to experimental infection by Paracoccidioides brasiliensis. Med Mycol. 2017;55(7).

54. Moon H-G, Yang J, Zheng Y, Jin Y. miR-15a/16 Regulates Macrophage Phagocytosis after Bacterial Infection. J Immunol. 2014;193(9).

55. de Araujo LS, Ribeiro-Alves M, Leal-Calvo T, Leung J, Durán V, Samir M, et al. Reprogramming of small noncoding RNA populations in peripheral blood reveals host biomarkers for latent and active mycobacterium tuberculosis infection. MBio. 2019;10(6).

56. Xu LJ, Jiang T, Zhao W, Han JF, Liu J, Deng YQ, et al. Parallel mRNA and microRNA profiling of HEV71-infected human neuroblastoma cells reveal the up-regulation of miR-1246 in association with DLG3 repression. PLoS One. 2014;9(4).

57. Guo L, Wang Q, Zhang D. MicroRNA-4485 ameliorates severe influenza pneumonia via inhibition of the STAT3/PI3K/AKT signaling pathway. Oncol Lett. 2020;20(5).

58. Lv J, Zhang Z, Pan L, Zhang Y. MicroRNA-34/449 family and viral infections. Vol. 260, Virus Research. 2019.

59. Dhorne-Pollet S, Crisci E, Mach N, Renson P, Jaffrézic F, Marot G, et al. The miRNA-targeted transcriptome of porcine alveolar macrophages upon infection with Porcine Reproductive and Respiratory Syndrome Virus. Sci Rep. 2019;9(1).

60. Oliver GF, Orang A V., Appukuttan B, Marri S, Michael MZ, Marsh GA, et al. Expression of microRNA in human retinal pigment epithelial cells following infection with Zaire ebolavirus. BMC Res Notes. 2019;12(1).

61. De Lacorte Singulani J, De Fátima Da Silva J, Gullo FP, Costa MC, Fusco-Almeida AM, Enguita FJ, et al. Preliminary evaluation of circulating microRNAs as potential biomarkers in paracoccidioidomycosis. Biomed Reports. 2017;6(3).

62. Singulani J de L, da Silva J de F, Gullo FP, Costa MC, Fusco-Almeida AM, Enguita FJ, et al. Fungal-host interactions: Insights into microRNA in response to paracoccidioides species. Mem Inst Oswaldo Cruz. 2020;115(7).

63. Cer RZ, Herrera-Galeano JE, Frey KG, Schully KL, Luu T V., Pesce J, et al. Differential MicroRNA Analyses of Burkholderia pseudomallei - and Francisella tularensis -Exposed hPBMCs Reveal Potential Biomarkers. Int J Genomics. 2017;2017.

64. Medina L, Castillo C, Liempi A, Guerrero-Muñoz J, Rojas-Pirela M, Maya JD, et al. Trypanosoma cruzi and Toxoplasma gondii Induce a Differential MicroRNA Profile in Human Placental Explants. Front Immunol. 2020;11:2864.

65. Louten J, Beach M, Palermino K, Weeks M, Holenstein G. MicroRNAs expressed during viral infection: Biomarker potential and therapeutic considerations. Vol. 10, Biomarker Insights. 2016.

66. Biswas S, Chen E, Haleyurgirisetty M, Lee S, Hewlett I, Devadas K. Comparison of miRNA expression profiles between HIV-1 and HIV-2 infected monocyte-derived macrophages (MDMs) and peripheral blood mononuclear cells (PBMCs). Int J Mol Sci. 2020;21(18).

67. Tamgue O, Gcanga L, Ozturk M, Whitehead L, Pillay S, Jacobs R, et al. Differential targeting of c-Maf, Bach-1, and Elmo-1 by microRNA-143 and microRNA-365 promotes the intracellular growth of mycobacterium tuberculosis in alternatively IL-4/IL-13 activated macrophages. Front Immunol. 2019;10(MAR).

68. Tambyah PA, Ching CS, Sepramaniam S, Ali JM, Armugam A, Jeyaseelan K. microRNA expression in blood of dengue patients. Ann Clin Biochem. 2015;53(4).

69. Budak F, Bal SH, Tezcan G, Akalin H, Goral G, Oral HB. Altered Expressions of miR-1238-3p, miR-494, miR-6069, and miR-139-3p in the Formation of Chronic Brucellosis. J Immunol Res. 2016;2016.

70. Bai L, Wang H, Wang AH, Zhang LY, Bai J. MicroRNA-532 and microRNA-3064 inhibit cell proliferation and invasion by acting as direct regulators of human telomerase reverse transcriptase in ovarian cancer. PLoS One. 2017;12(3).

71. Kan XQ, Li YB, He B, Cheng SF, Wei YJ, Sun J. Mir-1294 acts as a tumor inhibitor in cervical cancer by regulating flot1 expression. J Biol Regul Homeost Agents. 2020;34(2).

72. Zhang M, Wang F, Zhang X. miRNA-627 inhibits cell proliferation and cell migration, promotes cell apoptosis in prostate cancer cells through upregulating MAP3K1, PTPRK and SRA1. Int J Clin Exp Pathol. 2018;11(1):255.

73. Wang Y, Zhang S, Bao H, Mu S, Zhang B, Ma H, et al. MicroRNA-365 promotes lung carcinogenesis by downregulating the USP33/SLIT2/ROBO1 signalling pathway. Cancer Cell Int. 2018;18(1).

74. Nezu Y, Hagiwara K, Yamamoto Y, Fujiwara T, Matsuo K, Yoshida A, et al. MiR-135b, a key regulator of malignancy, is linked to poor prognosis in human myxoid liposarcoma. Oncogene. 2016;35(48).

75. Cao Z, Zhang G, Xie C, Zhou Y. Mir-34b regulates cervical cancer cell proliferation and apoptosis. Artif Cells, Nanomedicine Biotechnol. 2019;47(1).

76. Kharadi U, Kharadi UA, Parkarwar P, Khairnar S, Reddy S, Arur P. Oral Candidiasis Turns to Oral Cancer–A Rare Clinical Presentation. Clin Oncol. 2016;1:1126.

77. Bakri MM, Hussaini HM, Holmes A, Cannon RD, Rich AM. Revisiting the association between candidal infection and carcinoma, particularly oral squamous cell carcinoma. J Oral Microbiol. 2010;2(2010).

78. Williamson MK, Coombes N, Juszczak F, Athanasopoulos M, Khan MB, Eykyn TR, et al. Upregulation of glucose uptake and hexokinase activity of primary human CD4+ T cells in response to infection with HIV-1. Viruses. 2018;10(3).

79. Freeman BD, Machado FS, Tanowitz HB, Desruisseaux MS. Endothelin-1 and its role in the pathogenesis of infectious diseases. Vol. 118, Life Sciences. 2014.

80. Zambreg I, Assouline B, Housset C, Schiffer E. Overexpression of TGF-α and EGFR, a key event in liver carcinogenesis, is induced by hypoxia specifically in hepatocytes. Gastroenterol Hepatol Endosc. 2019;4(3).

81. Hawkins PT, Stephens LR. PI3K signalling in inflammation. Vol. 1851, Biochimica et Biophysica Acta - Molecular and Cell Biology of Lipids. 2015.

82. Zhu M, Yang H, Chen Z, Xia X, Deng Q, Shen Y. A cell-permeable peptide inhibitor of p55PIK signaling alleviates ocular inflammation in mouse models of uveitis. Exp Eye Res. 2020;199.

83. Lee HS, Woo SJ, Koh HW, Ka SO, Zhou L, Jang KY, et al. Regulation of apoptosis and inflammatory responses by insulin-like growth factor binding protein 3 in fibroblast-like synoviocytes and experimental animal models of rheumatoid arthritis. Arthritis Rheumatol. 2014;66(4).

84. Kim G-D, Ng HP, Chan ER, Mahabeleshwar GH. Kruppel-like factor 6 promotes macrophage inflammatory and hypoxia response. FASEB J Off Publ Fed Am Soc Exp Biol. 2020 Feb;34(2):3209–23.

85. Yasuoka H, Yamaguchi Y, Feghali-Bostwick CA. The pro-fibrotic factor IGFBP-5

induces lung fibroblast and mononuclear cell migration. Am J Respir Cell Mol Biol. 2009;41(2).

86. Dongari-Bagtzoglou A, Kashleva H. Candida albicans triggers interleukin-8 secretion by oral epithelial cells. Microb Pathog. 2003 Apr;34(4):169–77.

87. Spohn R, Daruka L, Lázár V, Martins A, Vidovics F, Grézal G, et al. Integrated evolutionary analysis reveals antimicrobial peptides with limited resistance. Nat Commun. 2019;10(1).

88. Kim D, Langmead B, Salzberg SL. HISAT: A fast spliced aligner with low memory requirements. Nat Methods. 2015;

89. Love MI, Huber W, Anders S. Moderated estimation of fold change and dispersion for RNA-seq data with DESeq2. Genome Biol. 2014;

90. Friedländer MR, MacKowiak SD, Li N, Chen W, Rajewsky N. MiRDeep2 accurately identifies known and hundreds of novel microRNA genes in seven animal clades. Nucleic Acids Res. 2012;40(1).

91. Yu G, Wang L-G, Yan G-R, He Q-Y. DOSE: an R/Bioconductor package for disease ontology semantic and enrichment analysis. Bioinformatics. 2014 Oct 17;31(4):608–9.

92. Yu G, Wang LG, Han Y, He QY. ClusterProfiler: An R package for comparing biological themes among gene clusters. Omi A J Integr Biol. 2012;

93. Carlson M, Falcon S, Pages H, Li N. org. Hs. eg. db: Genome wide annotation for Human. R Packag version. 2013;3(1).

94. Krämer A, Green J, Pollard J, Tugendreich S. Causal analysis approaches in ingenuity pathway analysis. Bioinformatics. 2014 Feb 15;30(4):523–30.